

RESEARCH ARTICLE

[View Article Online](#)
[View Journal](#) | [View Issue](#)

 Cite this: *Inorg. Chem. Front.*, 2023, **10**, 2088

Ionic Fe(III)-porphyrin frameworks for the one-pot synthesis of cyclic carbonates from olefins and CO₂†

 Rajesh Das,  Sahil Kamra and C. M. Nagaraja *

In this study, the rational construction of Fe^{III}-centered porphyrin-based bifunctional ionic porous organic polymers (**Fe-IPOP1/2**) for a one-step, halogen-free, cascade transformation of olefins and CO₂ to cyclic carbonates as compared to the conventional two-step process involving epoxides is presented. The ionic polymers, **Fe-IPOP1/2** showed selective and recyclable uptake of CO₂ with an interaction energy of 32.2/39.6 kJ mol⁻¹ signifying the stronger interaction of carbon dioxide with the frameworks. Both the polymers were found to be thermally stable up to 300 °C and exhibited promising catalytic performance in the one-step, halogen-free synthesis of cyclic carbonates under eco-friendly, cocatalyst/solvent-free, atmospheric pressure conditions. The excellent catalytic activity of **Fe-IPOP1/2** for a one-pot synthesis of cyclic carbonates has been ascribed to the presence of highly exposed oxophilic Fe^{III} sites and nucleophilic Br⁻ anions in the polymers. Notably, this one-pot synthesis strategy was extended for the transformation of various substituted olefins to their respective carbonates in good yield and selectivity. Further, **Fe-IPOP1** showed good reusability with retention of catalytic activity for multiple cycles of usage.

Received 5th December 2022

Accepted 23rd February 2023

DOI: 10.1039/d2qi02599j

rsc.li/frontiers-inorganic

Introduction

The major contributor to global climate destabilization is anthropogenic and naturally emitted carbon dioxide (CO₂), whose concentration is increasing day by day exceeding 400 ppm, currently.¹ This significant rise in CO₂ concentration in the atmosphere has been attributed to greater consumption of fossil fuels leading to major environmental issues like unpredictable weather patterns, global warming, ocean acidification, and so on.^{2–4} To overcome this, carbon capture,⁵ storage, and utilization have been adopted globally to contain the increasing CO₂ levels in the atmosphere.^{6–14} Given the plentiful amount of CO₂ in the atmosphere, its use as a non-toxic, abundant, and cheap C1-feedstock for value-added chemical and fuel production has become a major topic of interest for many researchers worldwide.^{15–21} In this direction, numerous strategies have been used for the utilization of CO₂ to obtain value-added chemicals.^{22–29} Among them, production of cyclic carbonates by the functionalization of epoxides using CO₂ has gained special interest due to its absolute atom economy.^{30–35} Notably, cyclic carbonates are of potential utility as precursors of polymeric materials, raw materials of pharmaceuticals and cosmetics, electrolytes in batteries, and

so on.^{36–39} Generally, cyclic carbonates have been synthesised by coupling CO₂ with epoxides.^{40–43} However, a one-pot reaction utilizing readily available olefins and CO₂ is an attractive eco-friendly strategy for the green synthesis of cyclic carbonates as compared to the conventional two-step process *via* the use of epoxides. Here, the catalyst employed needs to be highly reactive to catalyze the one-pot synthesis through the *in situ* formation of epoxides. For efficient, one-step transformation of olefins to cyclic carbonates, the catalyst should have a Lewis acidic, oxophilic metal ion such as Mn, Ti, Fe, Mo, *etc.* for the *in situ* formation of epoxides, which is favored due to the participation of the metal–oxo intermediate.^{44–47} In this direction, Fe-based catalysts have attracted significant interest due to their low cost, high abundance, and non-toxicity along with facile formation of Fe^{IV}=O active species during the reaction. More importantly, most of the catalysts reported for the synthesis of cyclic carbonates require an additional nucleophilic cocatalyst (halide ions) for facilitating ring-opening of the epoxide step. However, green chemistry practices demand that the synthesis be carried out under environment-friendly and halide-free mild conditions. In this regard, herein we report the strategic construction of bifunctional ionic porous organic polymers, **Fe-IPOP1/2**, by a polymerization reaction of Fe^{III}-TPyP (TpyP = 5,10,15,20-tetrakis(4-pyridyl)-porphyrin) with 1,4-bis(bromomethyl)benzene/4,4'-bis(bromomethyl)biphenyl, respectively, under an inert atmosphere. Indeed, **Fe-IPOP1/2** showed halogen-free CO₂ fixation activity with olefins under environment-friendly mild conditions. Furthermore, the role of Lewis acidic/oxophilic Fe^{III} sites was studied by preparing

Department of Chemistry, Indian Institute of Technology Ropar, Rupnagar-140001, Punjab, India. E-mail: cmnraja@iitrpr.ac.in; Tel: +91-1881-242229

† Electronic supplementary information (ESI) available: Synthesis procedures, FTIR plots, UV-Vis spectra, and ¹H NMR spectra of the catalytic reactions. See DOI: <https://doi.org/10.1039/d2qi02599j>

an analogous ionic polymer (**Zn-IPOP1**) using a Zn-TPyP metalloligand. Interestingly, **Zn-IPOP1** did not show catalytic activity for the one-step synthesis of cyclic carbonates highlighting the need for oxophilic Fe^{III} sites for the one-step cyclic carboxylation of olefins. Moreover, the role of nucleophilic Br⁻ ions in halide-free cyclic carbonates synthesis was studied by preparing an analogous non-ionic polymer (**Fe-POP1**). Overall, this is a rare demonstration of the application of an ionic porphyrin-based polymer for the halogen-free utilization of CO₂ in a one-pot reaction of CO₂ with olefins.

Results and discussion

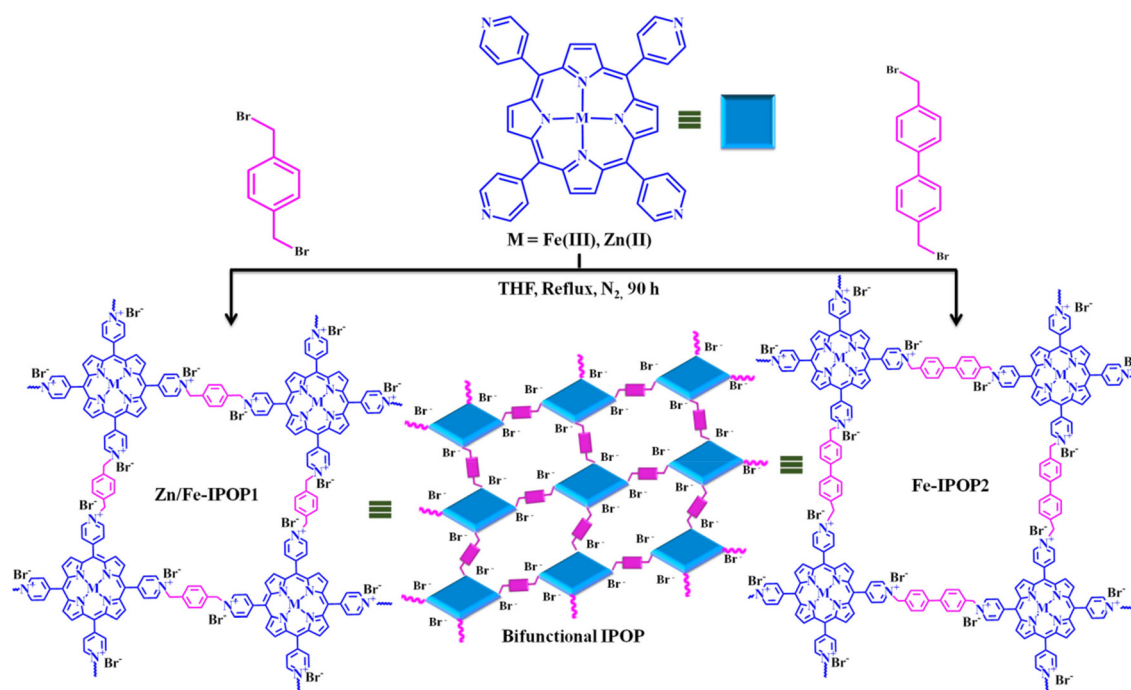
Synthesis and characterization

The 5,10,15,20-tetrakis(4'-pyridyl)porphyrin (TPyP) and metallated M-TPyP (M = Zn^{II}, Fe^{III}) ligand were prepared by following a reported procedure with a slight modification (see the ESI, Scheme S1†) and characterized by ¹H NMR, UV-Vis, and FTIR analysis (Fig. S1–S4†). The metallated porphyrin-based ionic polymers (**Zn/Fe-IPOP1**) were synthesized by the polymerization reaction of Zn/Fe-TPyP with 1,4-bis(bromomethyl)benzene. However, **Fe-IPOP2** was synthesized by reaction of Fe-TPyP with the 4,4'-bis(bromomethyl)biphenyl linker under an inert atmosphere as shown in Scheme 1. Furthermore, to test the role of nucleophilic Br⁻ ions on the halogen-free preparation of cyclic carbonates, an analogous non-ionic polymer (**Fe-POP**) was synthesized (please refer to the ESI†).⁴⁹

The incorporation of a Zn^{II}/Fe^{III} ion into the porphyrin ring was confirmed by the complete absence of pyrrolic N–H peaks

($\delta = -2.83$ ppm) of the porphyrin ring in the ¹H NMR spectrum (Fig. S2†). In addition, FTIR spectra of the M-TPyP complex showed the absence of N–H stretching frequencies at 3306 cm⁻¹ supporting the incorporation of metal ions (Fig. S3†). The UV-Vis spectra of the TPyP ligand showed an intense Soret band at 418 nm [a_{1u} → e_g] with four Q bands [a_{2u} → e_g (forbidden)] at 515, 550, 592, and 648 nm (Fig. S4†). The metallation of the TPyP ligand led to a redshift in the Soret band to 428 nm and also the number of Q bands was reduced to two (560 and 600 nm) due to the symmetry change of the molecule to D_{4h} further supporting the metallation of the porphyrin ring (Fig. S4†).

The PXRD plots of **Zn/Fe-IPOP1** and **Fe-IPOP2** showed a broad peak in the 2 θ region of 20–27° due to π - π stacking of porphyrin rings (Fig. S5†). New stretching frequencies at 1160 and 1629 cm⁻¹ appeared in the FT-IR spectra, which were assigned to alkyl C–N and the pyridine iminium ion (–C=N⁺), respectively, indicating the formation of an ionic polymer (Fig. S6 and S7†).^{48,50} Furthermore, an additional peak due to the aliphatic C–H stretching frequency at 2978 cm⁻¹ supporting the presence of methylene groups in the polymer was observed (Fig. S6 and S7†).⁵¹ The formation of **Zn-IPOP1** was also supported by solid-state ¹³C cross-polarized magic angle spinning (CP-MAS) NMR spectra (Fig. 1a). The methylene carbon (¹³CH₂) linked to the quaternary pyridyl ammonium showed resonance at a chemical shift (δ) of 63 ppm (¹³C_a) supporting the formation of the ionic polymer. The porphyrin ring carbon linked to the pyridyl ring (¹³C_g) showed resonance peaks at δ 119 ppm while the pyridyl ring carbon (¹³C_b) connected to the porphyrin ring was observed at



Scheme 1 Synthesis scheme for Zn/Fe-IPOP1 and Fe-IPOP2.

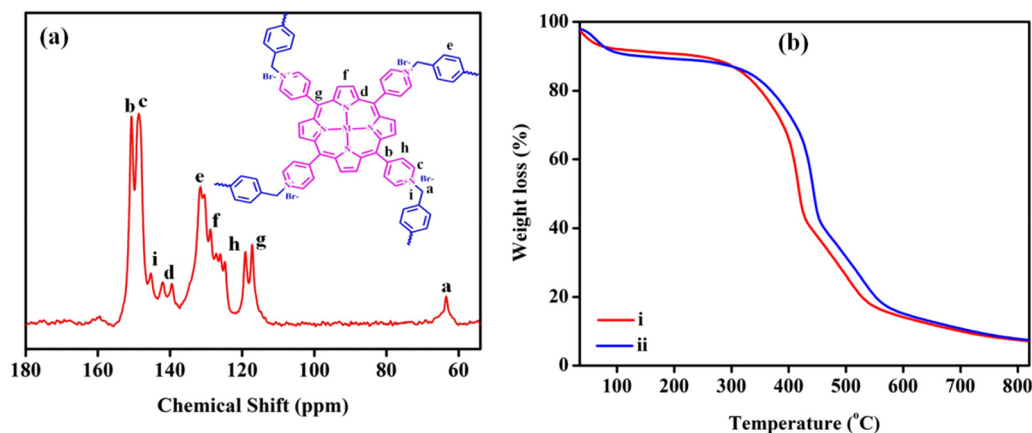


Fig. 1 (a) ^{13}C CP-MAS NMR spectra, and (b) TGA plot for Fe-IPOP1 (i) and Fe-IPOP2 (ii).

152 ppm.⁵² The pyrrole ring carbons ($^{13}\text{C}_f$ and $^{13}\text{C}_d$) appear at δ 131 and 145 ppm, respectively. The carbons ($^{13}\text{C}_h$ and $^{13}\text{C}_c$) of the pyridyl ring appeared at 129 and 148 ppm, respectively.⁴⁹ The phenyl ring carbon ($^{13}\text{C}_e$) showed a resonance peak at 132 ppm.⁴⁹

The thermal stability of the polymers was examined by thermogravimetric analysis (TGA). Fe-IPOP1/2 showed a weight loss of ~11% in the temperature range between RT and 90 $^{\circ}\text{C}$ corresponding to the loss of adsorbed solvent (acetone) molecules (Fig. 1b). Both Fe-IPOPs exhibited thermal stability up to 300 $^{\circ}\text{C}$, similar to that of Zn-IPOP1.⁴⁹ Furthermore, SEM analysis showed spherical morphology for Fe-IPOP1/2 (Fig. S8 \dagger). The energy dispersive spectroscopy (EDS) analysis of Fe-IPOP1 revealed the presence of constituent elements in the polymer (Fig. S9 \dagger).

X-ray photoelectron spectroscopy (XPS) analysis of Fe-IPOP1/2 was performed to confirm the presence of their constituent elements. The survey spectra of Fe-IPOP1 confirmed the presence of elemental Fe, Cl, Br, C, and N (Fig. S10 \dagger). The Fe-spectra show peaks with binding energy (BE) values of 710.7 and 724.7 eV assigned to $2p_{3/2}$ and $2p_{1/2}$, respectively (Fig. 2a). Interestingly, the observed BE for Fe^{III} matches well with the reported value for the Fe^{III}-centered porphyrin ring, affirming the incorporation of Fe^{III} in the porphyrin core.^{53,54} Furthermore, Cl spectra show BE peaks at 197.8 and 199.3 eV assigned to $2p_{3/2}$ and $2p_{1/2}$, which supports the coordination of the $-\text{Cl}$ ion to the Fe^{III} center (Fig. 2b).⁵³ Furthermore, the N spectra showed two BE peaks at 398.3 and 400.6 eV due to pyrrolic nitrogen (N_p1s) of the porphyrin ring and a quaternary nitrogen (N_q1s), respectively, which confirms the formation of

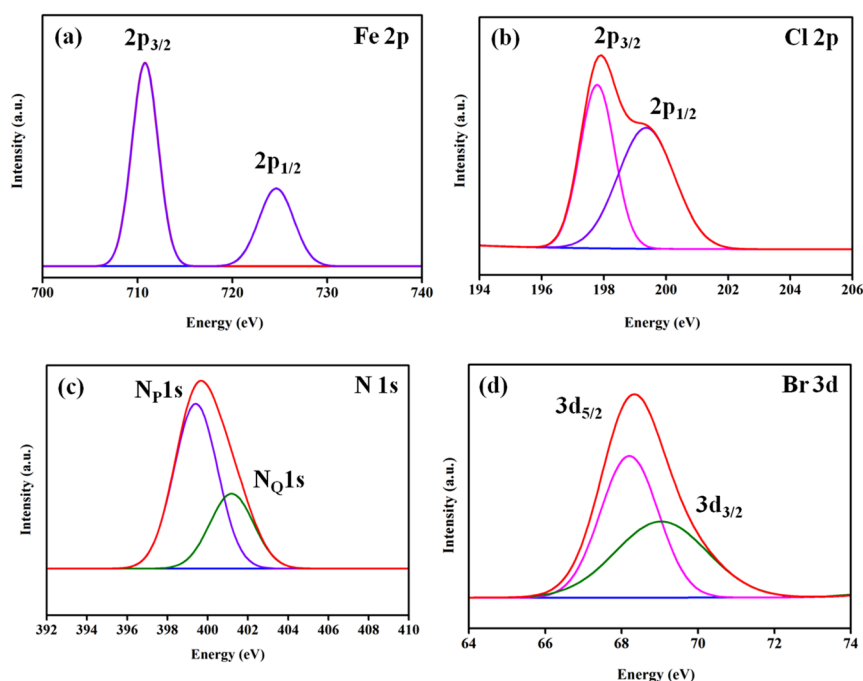


Fig. 2 XPS of Fe-IPOP2: (a) Fe 2p, (b) Cl 2p, (c) N 1s, and (d) Br 3d spectra.

the ionic polymer (Fig. 2c). The Br spectra show the appearance of two BE peaks at 68.2 and 69.1 eV assigned to $5d_{5/2}$ and $5d_{3/2}$, respectively (Fig. 2d). Similarly, XPS analysis of **Fe-IPOP2** confirmed the presence of its constituent elements (Fig. S11†). The Fe spectra show BE peaks at 711.1 and 724.8 eV assigned to $2p_{3/2}$ and $2p_{1/2}$, respectively (Fig. S11†). However, the Cl spectra depict peaks at 197.9 and 199.5 eV, due to $2p_{3/2}$ and $2p_{1/2}$, respectively, and the N and Br spectra (Fig. S11†) are found to be similar to those of **Fe-IPOP1** affirming the isostructural nature of **Fe-IPOP1/2**.

Gas adsorption studies

N_2 adsorption of **Fe-IPOP1/2** was measured to determine the porosity of the ionic polymers. The estimated BET surface area of **Fe-IPOP1** ($26.5 \text{ m}^2 \text{ g}^{-1}$) was found to be in close agreement with the value reported for isostructural **Zn-IPOP1** ($16 \text{ m}^2 \text{ g}^{-1}$) (Fig. S12†), whereas **Fe-IPOP2** showed a relatively higher BET surface area of $77.5 \text{ m}^2 \text{ g}^{-1}$ (Fig. S13†). Furthermore, pore size distribution analysis of **Fe-IPOP1/2** revealed pore sizes of 6.1/8.3 Å, respectively. The relatively larger pore size in **Fe-IPOP2** has been ascribed to the presence of the longer linker of 4,4'-bis(bromomethyl)biphenyl (7.2 Å) rather than 1,4-bis(bromomethyl)benzene (5.3 Å) used in **Fe-IPOP1** (Fig. S14†). Furthermore, to test the CO_2 -philicity of **Fe-IPOP1/2**, gas sorption studies were carried out. As can be seen from Fig. 3, both **Fe-IPOP1/2** showed type-I isotherms with uptake of 40.6/28.6 and 64.4/43.9 cc g^{-1} at 273 and 298 K, respectively (Fig. 3a and b). The relatively higher CO_2 uptake of **Fe-IPOP2** as compared to that of **Fe-IPOP1** can be correlated to its higher surface area/

porosity. Furthermore, the accurate prediction of CO_2 uptake was carried out by adopting the Freundlich–Langmuir equation⁵⁵ (Fig. S15 and S18†) and the adsorption energy (Q_{st}) was determined from the Clausius–Clayperon equation.⁵⁶ Interestingly, the Q_{st} for CO_2 with **Fe-IPOP1/2** was calculated and found to be 32.2/39.6 kJ mol^{-1} signifying the stronger interaction of carbon dioxide with the frameworks (Fig. S19 and S20†). Additionally, selective gas sorption measurements (Fig. 3c) revealed negligible uptake of N_2 , and CH_4 with relatively high Henry gas selectivity constants of 71 and 69 for $K_{\text{CO}_2/\text{N}_2}$ and $K_{\text{CO}_2/\text{CH}_4}$, respectively (Fig. S21†). Notably, **Fe-IPOP1** showed recyclable CO_2 adsorption properties (Fig. 3d). Furthermore, the basic and acidic strengths of **Fe-IPOP1** quantified by CO_2 and NH_3 TPD (temperature-programmed desorption) analysis were found to be 0.46 and 0.53 mmol g^{-1} , respectively (Fig. S22†). Thus, the TPD analysis revealed the bifunctional nature of **Fe-IPOP1** having moderate basic and acidic sites, which is an essential requirement for effective transformation of CO_2 under mild conditions.

Catalytic epoxidation reaction of olefins to epoxides

The presence of oxophilic/Lewis acidic Fe^{III} and nucleophilic (Br^-) sites in **Fe-IPOP1/2** motivated us to test their catalytic performance for one-pot, halogen-free fixation of readily available olefins with CO_2 to produce valuable feedstocks, that is cyclic carbonates. It is worth noting that the majority of reports on cyclic carbonates describe utilizing epoxides, which are prepared by the epoxidation of olefins catalyzed by Lewis acidic metal ions.^{57–61} Hence, to establish the formation of an

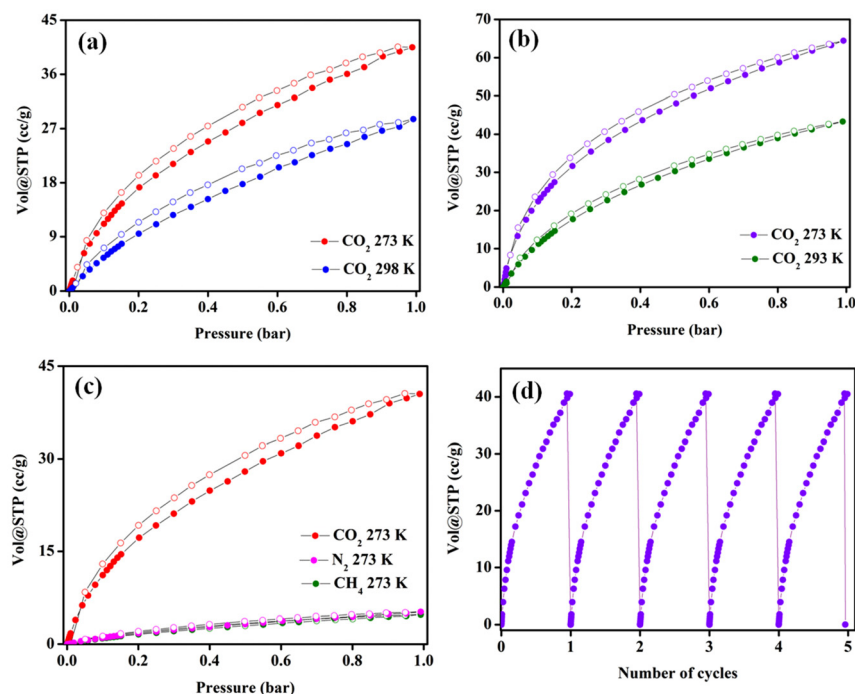


Fig. 3 CO_2 adsorption isotherms for (a) **Fe-IPOP1** and (b) **Fe-IPOP2**. (c) Selective CO_2 adsorption isotherm, and (d) recyclable CO_2 adsorption for **Fe-IPOP1**.

epoxide as an intermediate *en route* to the formation of cyclic carbonates, the catalytic activity of **Fe-IPOP1/2** was tested for the generation of epoxides from olefins using PhIO as an oxidizing agent at RT. The catalytic conditions were optimized using styrene as a model substrate by varying the reaction parameters (Table S1†). Notably, both **Fe-IPOP1/2** catalyzed the epoxidation of styrene to yield styrene oxide (SO) with more than 99% yield within 18 h at RT with 100% selectivity (Table 1 and Fig. S23, S24†). Furthermore, to check the role of Fe^{III} ions in catalyzing the epoxidation reaction, a control experiment was carried out using analogous Zn-centered porphyrin POP (**Zn-IPOP1**) as a catalyst. To our delight, negligible conversion (<5%) of styrene to SO was observed under the optimized conditions (Fig. S25†). This study highlights the importance of oxophilic Fe^{III} ions for the oxidation of olefins to epoxides. Furthermore, the catalytic study was extended to the oxidation of various olefins including both substituted sty-

renes and linear alkenes (Table 1). Interestingly, most of the olefins were found to undergo conversion to their respective oxides with high yield and selectivity (Table 1).

One-step cyclic carbonate synthesis from olefins and CO₂

The high catalytic activity of **Fe-IPOP1/2** towards epoxidation of both aromatic and aliphatic olefins motivated us to test their catalytic performance for one-pot cyclic carbonate synthesis using readily accessible olefins and CO₂ (Fig. 4a). To start with, the catalysis was performed using styrene as a model substrate and the reaction conditions were optimized by varying the temperature and time of reaction (Fig. 4 and Table S2†). Under the optimized reaction conditions, **Fe-IPOP1** catalyzed the one-step oxidative carboxylation of styrene to styrene carbonate (SC) with >99% conversion within 24 h under halogen-free mild conditions of 1 atm of CO₂ (Fig. 4 and S26, S27, Table S2†). Furthermore, controlled experiments performed

Table 1 The catalytic activity of **Fe-IPOP1/2** for epoxidation of olefins^a

S. no.	Substrate	Product	Catalyst	Conversion (%) ^b	TON ^c
1			Zn-IPOP1	—	—
2			Fe-IPOP1	>99	143
3			Fe-IPOP2	>99	140
4			Fe-IPOP1	95	136
5			Fe-IPOP1	89	127
6			Fe-IPOP1	83	119
7			Fe-IPOP1	78	111
8			Fe-IPOP1	76	109
9			Fe-IPOP1	71	101
10			Fe-IPOP1	66	94

^a Reaction conditions: olefin (1 mmol), catalyst (10 mg), PhIO (1.5 mmol), temperature (25 °C), and time (18 h). ^b The catalytic conversion was determined by ¹H NMR analysis. ^c TON = number of mmol of product formed/number of mmol catalyst used.

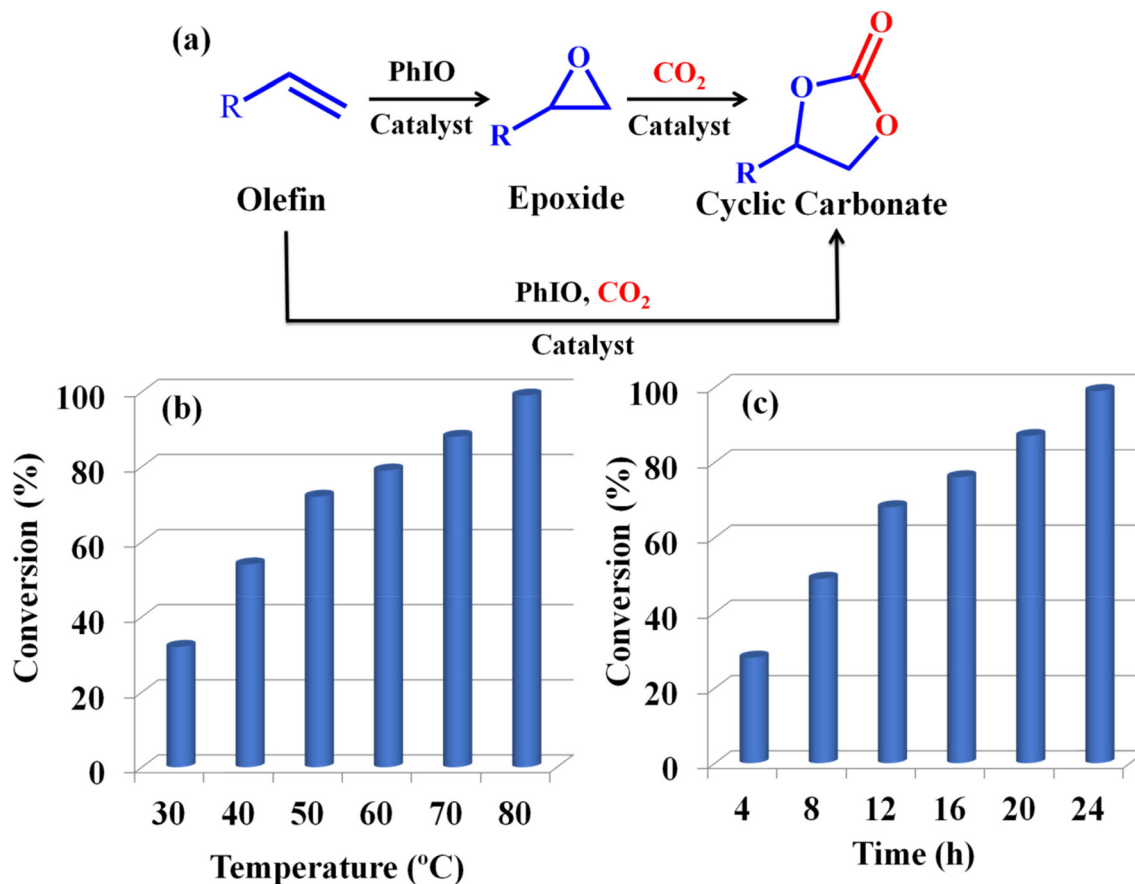


Fig. 4 (a) Catalytic one-pot synthesis of cyclic carbonates. Optimization of the catalytic reaction by varying the temperature (b) and time (c).

using polymer precursors *i.e.* Fe-TPyP, 1,4-bis(bromomethyl) benzene, 4,4'-bis(bromomethyl)biphenyl and FeCl₃ did not show styrene carbonate formation (Table S2†), highlighting the essential requirement of **Fe-IPOP1** for generating cyclic carbonates from olefins and CO₂. Thus, the control experiments revealed that for one-pot, halogen-free transformation of CO₂ to cyclic carbonates both oxophilic metal and nucleophilic halogen sites are essential. In the case of Fe-TPyP and FeCl₃ catalyzed reactions, although the presence of an oxophilic metal site is fulfilled, the nucleophilic Br⁻ sites are absent, which are necessary for promoting ring-opening of the epoxides and therefore results in no formation of cyclic carbonates. Furthermore, the catalytic activity carried out with **Fe-IPOP2** as the catalyst showed almost similar results to that of **Fe-IPOP1** with >99% conversion of styrene to SC (Fig. S28†). The efficient halogen-free catalytic activity of **Fe-IPOP1** was further extended for one-step cyclic carboxylation of various olefins including substituted styrenes and linear alkenes to their respective cyclic carbonates. Interestingly, **Fe-IPOP1** catalyzed the transformation of a series of olefins to cyclic carbonates under halogen-free optimized conditions and the catalytic conversions are summarized in Table 2 (Fig. S29–S32†). The relatively lower conversion of long-chain linear alkenes, say 1-hexene (73%), 1-octene (69%), and 1-decene (64%), has been ascribed to their bulkiness and lower π -electron density.⁶²

Notably, a comparison of the catalytic activity of **Fe-IPOP1** with reported systems revealed its superior performance for one-step cyclic carbonate synthesis from readily accessible olefin and CO₂ (Table 3).

Mechanistic investigation for one-step cyclic carboxylation of olefins

As discussed in the aforementioned section, the one-step cyclic carbonate synthesis from olefins and CO₂ proceeds through the formation of an epoxide intermediate. To establish the *in situ* formation of epoxide, the progress of the catalysis was monitored by a time-dependent ¹H NMR study. As shown in Fig. 5, ¹H NMR spectra of the aliquot taken at 6 h showed peaks corresponding to styrene oxide along with the product, styrene carbonate, and reactant, styrene (Fig. 5). Furthermore, as the reaction time increased to 18 h, the intensity of the peaks due to styrene oxide decreases and that of styrene carbonate increases, and at 24 h only peaks due to the SC are observed. This study unambiguously confirms the *in situ* generation of styrene oxide during the one-step cyclic carboxylation of olefins. Once the styrene oxide (epoxide) is formed, its coordination to a Lewis acidic (Fe^{III}) site leads to the polarization of the epoxide into which insertion of a CO₂ molecule takes place. Furthermore, to confirm the interaction of epoxide with the Fe^{III} site, a control experiment was carried

Table 2 Catalytic one-step synthesis of cyclic carbonates from olefin and CO₂^a

S. no.	Substrate	Product	Catalyst	Conversion ^c (%)	Selectivity for CC ^d	TON ^e
1			Zn-IPOP1	—	—	—
2			Fe-IPOP1	>99	96	137
3			Fe-IPOP2	>99	97	139
4			Fe-IPOP1	96	93	133
5			Fe-IPOP1	91	89	127
6			Fe-IPOP1	86	82	117
7			Fe-IPOP1	78	74	106
8			Fe-IPOP1	73	72	103
9			Fe-IPOP1	69	67	96
10			Fe-IPOP1	64	62	89
11 ^b			Fe-POP	>99	97	138

^a Reaction conditions: olefin (1 mmol), catalyst (10 mg), PhIO (1.5 mmol), CO₂ (1 bar), DCM (2 mL), temperature (80 °C), and time (24 h).

^b Catalyst (non-ionic polymer), **Fe-POP** (10 mg). ^c Catalytic conversion was determined by ¹H NMR analysis. ^d The selectivity is calculated based on cyclic carbonate and the rest of the product corresponds to epoxide. ^e TON = number of mmol of product formed/number of mmol of catalyst used.

Table 3 Comparison of catalytic activity of **Fe-IPOP1** for one-step synthesis of styrene carbonates with that of literature-reported catalysts

S. no.	Catalyst	Co-catalyst	Pressure	Temperature (°C)	Conversion (%)	Ref.
1	ZnW PYIs14	TBABr	05	50	92	63
2	MOF-590	TBABr	01	80	93	64
3	MNP@SiO ₂ -8Mn	PPNCl	10	80	99	65
4	Ti-MMM-E	TBABr	08	70	92	66
5	Fe ^{III} @MOF1	TBABr	08	80	98.6	67
6	MOF-892	TBABr	01	80	51	68
7	ImBr-MOF-545(Mn)	—	05	70	99	59
8	Fe-IPOP1	Halogen free	01	80	99	This work

out in which **Fe-POP1** catalyst was treated with epoxide (styrene oxide) for 2 h and then the catalyst was recovered and washed thoroughly with methanol followed by drying at 80 °C under vacuum. The FT-IR spectra of the recovered sample showed peaks due to styrene oxide, supporting the polarization of styrene oxide at Fe^{III} sites (Fig. S33†). This step is followed

by ring-opening of SO by nucleophilic Br⁻ ions of the polymer. To support this step, an analogous polymer, **Fe-POP**, which lacks free Br⁻ ions, was synthesized (Scheme S2†) and its catalytic performance tested in the one-step cyclic carbonate synthesis under identical conditions.⁴⁸ To our delight, only styrene oxide (>99) formation was observed as opposed to

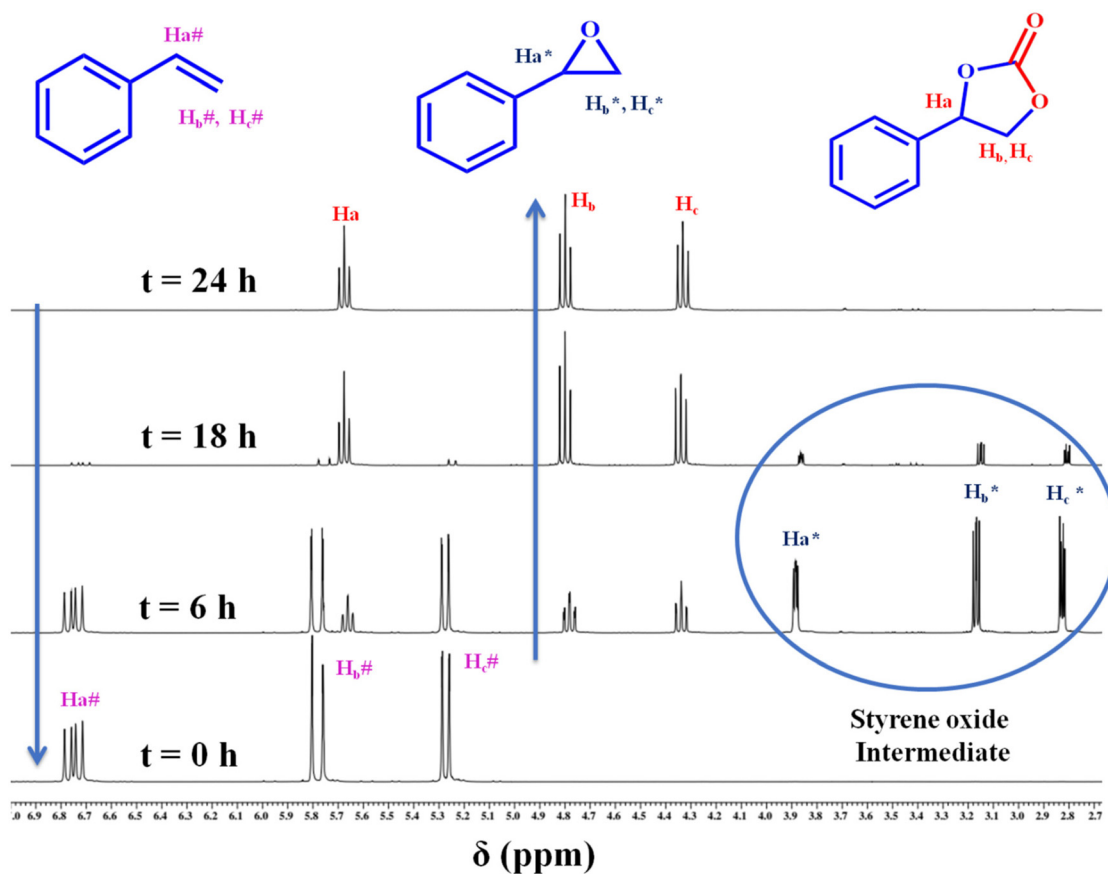
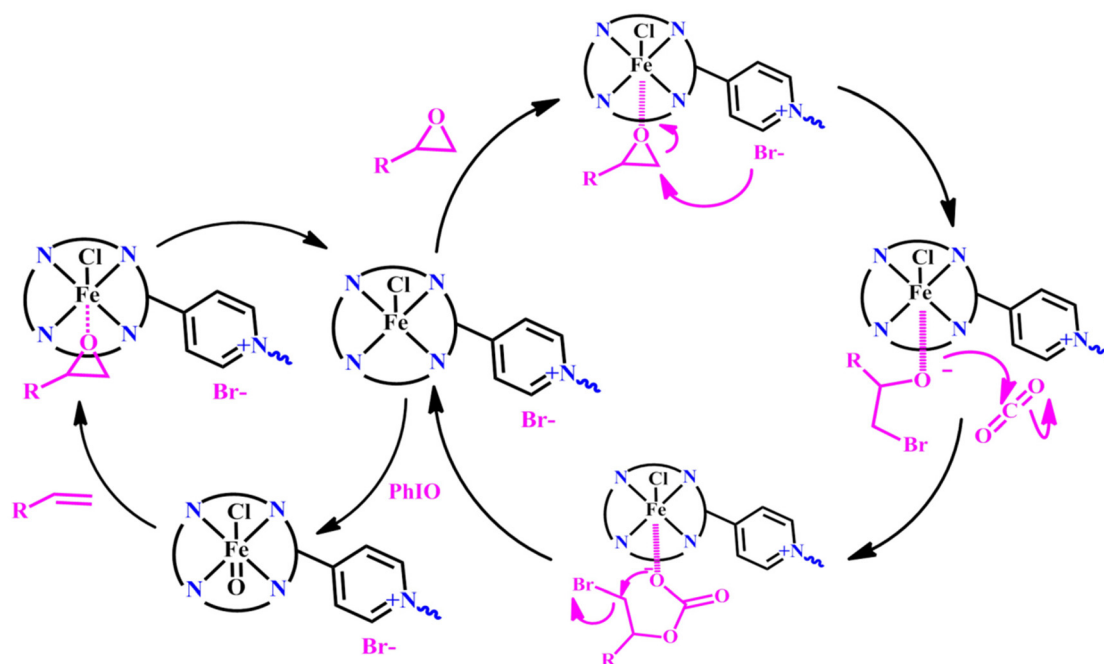


Fig. 5 Time-dependent ^1H NMR (400 MHz, CDCl_3 , 20 $^\circ\text{C}$) spectra for one-pot styrene carbonate synthesis.



Scheme 2 Plausible mechanism for catalytic one-pot reaction of CO_2 with an olefin to generate cyclic carbonates.

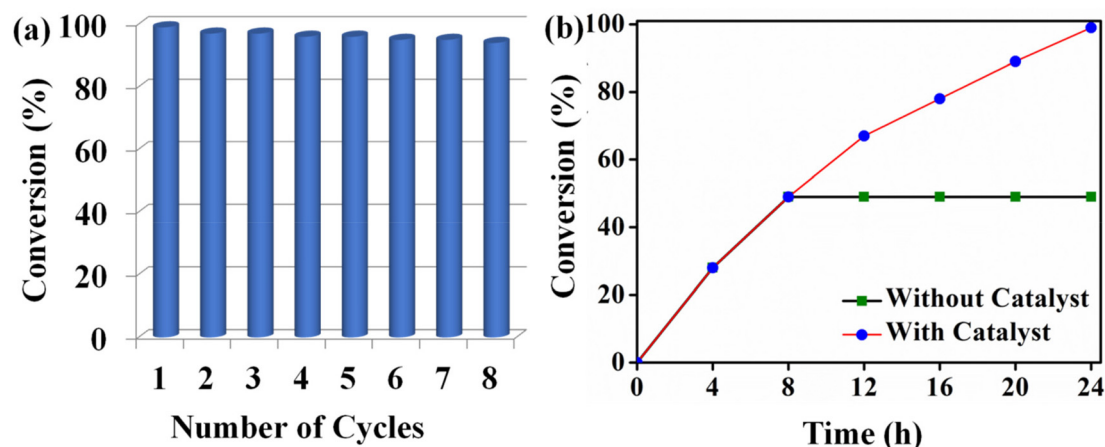


Fig. 6 (a) Catalyst reusability and (b) leaching test.

styrene carbonate formation as in the case of **Fe-POP1** (Table 2). However, the addition of a cocatalyst (2.5 mol% TBABr) to the reaction led to the formation of styrene carbonate. These studies brought out the essential requirement of a bifunctional catalyst composed of acidic and nucleophilic sites to achieve a one-step synthesis of cyclic carbonates under halogen-free conditions.

Based on the above discussion, the mechanism for the one-step cascade reaction of CO₂ with styrene catalyzed by a bifunctional **Fe-POP1** catalyst is shown in Scheme 2. The direct carboxylation of styrene proceeds with the *in situ* generation of styrene oxide by the oxidation of styrene. Then polarization of styrene oxide at the Fe^{III} sites, followed by its ring-opening upon nucleophilic attack of a Br⁻ anion, results in a bromoalkoxide intermediate. Then the subsequent addition of CO₂ produces metal carbonate species and its ring-closure reaction leads to styrene carbonate and its elimination regenerates the catalyst.

Recyclability and catalyst leaching test

Chemical stability and reusability are essential requirements for a heterogeneous catalyst. The reusability of **Fe-IPOP1** was investigated by isolating it from the reaction mixture followed by activation at 100 °C for 12 h. It is important to note that **Fe-IPOP1** was reusable for eight cycles with no significant loss of activity (Fig. 6a and S34[†]). Additionally, PXRD, FTIR, and XPS analyses of the regenerated polymer confirm its structural stability (Fig. S5, S35 and S36[†]). Furthermore, the BET surface area (22.3 m² g⁻¹) of the recycled sample was found to be almost close to that of the as-synthesized sample (26.5 m² g⁻¹), supporting retention of the original network structure even after eight catalytic cycles. To exclude any leaching of active metal (Fe^{III}) into the homogeneous system, the reaction was halted after 8 h and the catalyst was separated by filtration, and the reaction was continued for some more time. Surprisingly, no discernible rise in conversion was detected, indicating the absence of leaching of active species into solution (Fig. 6b). Furthermore, MP-AES analysis of the reaction fil-

trate showed no detectable Fe^{III} ions in the solution, which rule out any leaching during catalysis (Fig. S37[†]).

Conclusion

In summary, a strategic design of bifunctional Fe-porphyrin-based ionic POP by integrating oxophilic Fe sites and nucleophilic Br⁻ anions essential for the one-pot synthesis of cyclic carbonates under eco-friendly and halogen-free conditions is presented. The role of oxophilic and nucleophilic sites in catalytic activity was established. Importantly, **Fe-IPOP1** showed excellent reusability with retention of catalytic performance and structural integrity. This work constitutes the first demonstration of an ionic Fe-porphyrin polymer-catalyzed one-pot synthesis of cyclic carbonates from readily accessible olefins and carbon dioxide.

Conflicts of interest

The authors declare no conflict of interest.

Acknowledgements

CMN thanks the Science & Engineering Research Board (SERB), Department of Science and Technology, Govt. of India, for financial support (CRG/2018/001176). R. D. and S. K. thank IIT Ropar for their fellowships.

References

- 1 F. Joos, G.-K. Plattner, T. F. Stocker, O. Marchal and A. Schmittner, Global Warming and Marine Carbon Cycle Feedbacks on Future Atmospheric CO₂, *Science*, 1999, **284**, 464–467.

- 2 M. Z. Jacobson, Review of solutions to global warming, air pollution, and energy security, *Energy Environ. Sci.*, 2009, **2**, 148–173.
- 3 H. D. Matthews, T. L. Graham, S. Keverian, C. Lamontagne, D. Seto and T. J. Smith, National contributions to observed global warming, *Environ. Res. Lett.*, 2014, **9**, 014010.
- 4 W. D. Jones, Carbon Capture and Conversion, *J. Am. Chem. Soc.*, 2020, **142**, 4955–4957.
- 5 M. Wilson, S. N. Barrientos-Palomo, P. C. Stevens, N. L. Mitchell, G. Oswald, C. M. Nagaraja and J. P. S. Badyal, Substrate-Independent Epitaxial Growth of the Metal-Organic Framework MOF-508a, *ACS Appl. Mater. Interfaces*, 2018, **10**, 4057–4065.
- 6 R. Das and C. M. Nagaraja, Noble metal-free Cu(I)-anchored NHC-based MOF for highly recyclable fixation of CO₂ under RT and atmospheric pressure conditions, *Green Chem.*, 2021, **23**, 5195–5204.
- 7 A. Katelhon, R. Meys, S. Deutz, S. Suh and A. Bardow, Climate change mitigation potential of carbon capture and utilization in the chemical industry, *Proc. Natl. Acad. Sci. U. S. A.*, 2019, **116**, 11187–11194.
- 8 C. M. Nagaraja, R. Halder, T. K. Maji and C. N. R. Rao, Chiral Porous Metal-Organic Frameworks of Co(II) & Ni(II): Synthesis, Structure, Magnetic Properties and CO₂ Uptake, *Cryst. Growth Des.*, 2012, **12**, 975.
- 9 Q. Liu, L. Wu, R. Jackstell and M. Beller, Using carbon dioxide as a building block in organic synthesis, *Nat. Commun.*, 2015, **6**, 5933.
- 10 R. Das, T. Ezhil, A. S. Palakkal, D. Muthukumar, R. S. Pillai and C. M. Nagaraja, Efficient chemical fixation of CO₂ from direct air under environment-friendly co-catalyst and solvent-free ambient conditions, *J. Mater. Chem. A*, 2021, **9**, 23127–23139.
- 11 T. Sakakura, J. C. Choi and H. Yasuda, Transformation of Carbon Dioxide, *Chem. Rev.*, 2007, **107**, 2365–2387.
- 12 S. C. Peter, Reduction of CO₂ to Chemicals and Fuels: A Solution to Global Warming and Energy Crisis, *ACS Energy Lett.*, 2018, **3**, 1557–1561.
- 13 R. Das, S. S. Manna, B. Pathak and C. M. Nagaraja, Strategic Design of Mg-Centered Porphyrin Metal-Organic Framework for Efficient Visible Light-Promoted Fixation of CO₂ under Ambient Conditions: Combined Experimental and Theoretical Investigation, *ACS Appl. Mater. Interfaces*, 2022, **14**, 33285–33296.
- 14 T. K. Pal, D. De and P. K. Bharadwaj, Metal-organic frameworks as heterogeneous catalysts for the chemical conversion of carbon dioxide, *Fuel*, 2022, **320**, 123904.
- 15 W. D. Jones, Carbon Capture and Conversion, *J. Am. Chem. Soc.*, 2020, **142**, 4955–4957.
- 16 A. Katelhon, R. Meys, S. Deutz, S. Suh and A. Bardow, Climate change mitigation potential of carbon capture and utilization in the chemical industry, *Proc. Natl. Acad. Sci. U. S. A.*, 2019, **116**, 11187–11194.
- 17 B. Ugale, S. Kumar, T. J. D. Kumar and C. M. Nagaraja, Environmentally Friendly, Co-catalyst-Free Chemical Fixation of CO₂ at Mild Conditions Using Dual-Walled Nitrogen-Rich Three Dimensional Porous Metal–Organic Frameworks, *Inorg. Chem.*, 2019, **58**, 3925–3936.
- 18 Q. Liu, L. Wu, R. Jackstell and M. Beller, Using carbon dioxide as a building block in organic synthesis, *Nat. Commun.*, 2015, **6**, 5933.
- 19 T. Sakakura, J. C. Choi and H. Yasuda, Transformation of Carbon Dioxide, *Chem. Rev.*, 2007, **107**, 2365–2387.
- 20 R. Das, S. S. Dhankhar and C. M. Nagaraja, Construction of a bifunctional Zn(II)-organic framework containing basic amine functionality for selective capture and room temperature fixation of CO₂, *Inorg. Chem. Front.*, 2020, **7**, 72–81.
- 21 Y.-H. Zou, Y.-B. Huang, D.-H. Si, Q. Yin, Q.-J. Wu, Z. Weng and R. Cao, Porous Metal-Organic Framework Liquids for Enhanced CO₂ Adsorption and Catalytic Conversion, *Angew. Chem., Int. Ed.*, 2021, **60**, 20915.
- 22 X. L. Meng, Y. Nie, J. Sun, W. G. Cheng, J. Q. Wang, H. Y. He and S. J. Zhang, Superbase/cellulose: an environmentally benign catalyst for chemical fixation of carbon dioxide into cyclic carbonates, *Green Chem.*, 2014, **16**, 2771–2778.
- 23 R. Das, V. Parihar and C. M. Nagaraja, Strategic design of a bifunctional Ag(I)-grafted NHC-MOF for efficient chemical fixation of CO₂ from a dilute gas under ambient conditions, *Inorg. Chem. Front.*, 2022, **9**, 2583–2593.
- 24 Y. Mitsuka, N. Ogiwara, M. Mukoyoshi, H. Kitagawa, T. Yamamoto, T. Toriyama, S. Matsumura, M. Haneda, S. Kawaguchi, Y. Kubota and H. Kobayashi, Fabrication of Integrated Copper-Based Nanoparticles/Amorphous Metal–Organic Framework by a Facile Spray-Drying Method: Highly Enhanced CO₂ Hydrogenation Activity for Methanol Synthesis, *Angew. Chem., Int. Ed.*, 2021, **60**, 22283–22288.
- 25 M. SK, S. Barman, S. Paul, R. De, S. S. Sreejith, H. Reinsch, M. Grzywa, N. Stock, D. Volkmer, S. Biswas and S. Roy, An Anthracene-Based Metal-Organic Framework for Selective Photo-Reduction of Carbon Dioxide to Formic Acid Coupled with Water Oxidation, *Chem. – Eur. J.*, 2021, **27**, 4098–4107.
- 26 Y. Gu, M. Tamura, Y. Nakagawa, K. Nakao, K. Suzukic and K. Tomishige, Direct synthesis of polycarbonate diols from atmospheric flow CO₂ and diols without using dehydrating agents, *Green Chem.*, 2021, **23**, 5786–5796.
- 27 Q.-J. Wu, J. Liang, Y.-B. Huang and R. Cao, Thermo-, Electro-, and Photocatalytic CO₂ Conversion to Value Added Products over Porous Metal/Covalent Organic Frameworks, *Acc. Chem. Res.*, 2022, **55**, 2978–2997.
- 28 J. Liang, R.-P. Chen, X.-Y. Wang, T.-T. Liu, X.-S. Wang, Y.-B. Huang and R. Cao, Postsynthetic ionization of an imidazole-containing metal-organic framework for the cycloaddition of carbon dioxide and epoxides, *Chem. Sci.*, 2017, **8**, 1570–1575.
- 29 C. He, J. Liang, Y.-H. Zou, J.-D. Yi, Y.-B. Huang and R. Cao, Metal-organic frameworks bonded with metal N-heterocyclic carbenes for efficient catalysis, *Natl. Sci. Rev.*, 2022, **9**, 157.
- 30 J. Liang, Y.-B. Huang and R. Cao, Metal-organic frameworks and porous organic polymers for sustainable fixation

- of carbon dioxide into cyclic carbonates, *Coord. Chem. Rev.*, 2019, **378**, 32–65.
- 31 R. Das, D. Muthukumar, R. S. Pillai and C. M. Nagara, Rational Design of a Zn^{II} MOF with Multiple Functional Sites for Highly Efficient Fixation of CO₂ under Mild Conditions: Combined Experimental and Theoretical Investigation, *Chem. – Eur. J.*, 2020, **26**, 17445–17454.
- 32 M. Ding, R. W. Flaig, H.-L. Jiang and O. M. Yaghi, Carbon capture and conversion using metal–organic frameworks and MOF-based materials, *Chem. Soc. Rev.*, 2019, **48**, 2783–2828.
- 33 S. S. Dhankhar, B. Ugale and C. M. Nagaraja, Co-Catalyst-Free Chemical Fixation of CO₂ into Cyclic Carbonates by using Metal–Organic Frameworks as Efficient Heterogeneous Catalysts, *Chem. – Asian J.*, 2020, **15**, 2403–2427.
- 34 T. K. Pal, D. De and P. K. Bhardwaj, Metal–organic frameworks for the chemical fixation of CO₂ into cyclic carbonates, *Coord. Chem. Rev.*, 2020, **408**, 213173.
- 35 R. Das and C. M. Nagaraja, Highly Efficient Fixation of Carbon Dioxide at RT and Atmospheric Pressure Conditions: Influence of Polar Functionality on Selective Capture and Conversion of CO₂, *Inorg. Chem.*, 2020, **59**, 9765–9773.
- 36 B. Scrosati, J. Hassounab and Y.-K. Sun, Lithium-ion batteries. A look into the future, *Energy Environ. Sci.*, 2011, **4**, 3287–3295.
- 37 B. Grignard, S. Gennen, C. Jérôme, A. W. Kleij and C. Detrembleur, Advances in the use of CO₂ as a renewable feedstock for the synthesis of polymers, *Chem. Soc. Rev.*, 2019, **48**, 4466–4514.
- 38 H. Liu, S. Lin, Y. Feng and P. Theato, CO₂-Responsive polymer materials, *Polym. Chem.*, 2017, **8**, 12–23.
- 39 S. Fukuoka, M. Kawamura, K. Komiyama, M. Tojo, H. Hachiya, K. Hasegawa, M. Aminaka, H. Okamoto, I. Fukawad and S. Konno, A novel non-phosgene polycarbonate production process using by-product CO₂ as starting material, *Green Chem.*, 2003, **5**, 497–507.
- 40 S. Liu, H. Chen and X. Zhang, Bifunctional {Pb₁₀K₂}–Organic Framework for High Catalytic Activity in Cycloaddition of CO₂ with Epoxides and Knoevenagel Condensation, *ACS Catal.*, 2022, **12**, 10373–10383.
- 41 Y. B. N. Tran, P. T. K. Nguyen, Q. T. Luong and K. D. Nguyen, Series of M-MOF-184 (M = Mg, Co, Ni, Zn, Cu, Fe) Metal–Organic Frameworks for Catalysis Cycloaddition of CO₂, *Inorg. Chem.*, 2020, **59**, 16747–16759.
- 42 G. Zhai, Y. Liu, L. Lei, J. Wang, Z. Wang, Z. Zheng, P. Wang, H. Cheng, Y. Dai and B. Huang, Light-Promoted CO₂ Conversion from Epoxides to Cyclic Carbonates at Ambient Conditions over a Bi-Based Metal–Organic Framework, *ACS Catal.*, 2021, **11**, 1988–1994.
- 43 R. Das, T. Ezhil and C. M. Nagaraja, Design of Bifunctional Zinc(II)–Organic Framework for Efficient Coupling of CO₂ with Terminal/Internal Epoxides under Mild Conditions, *Cryst. Growth Des.*, 2022, **22**, 598–607.
- 44 G. De Faveri, G. Ilyashenko and M. Watkinson, Recent advances in catalytic asymmetric epoxidation using the environmentally benign oxidant hydrogen peroxide and its derivatives, *Chem. Soc. Rev.*, 2011, **40**, 1722–1760.
- 45 N. Anbazhagan, G. Imran, A. Qurashi, A. Pandurangan and S. Manimaran, Confinement of Mn³⁺ redox sites in Mn-KIT-6 and its catalytic activity for styrene epoxidation, *Microporous Mesoporous Mater.*, 2017, **247**, 190–197.
- 46 S. Rayati, P. Nafarieh and M. M. Amini, The synthesis, characterization and catalytic application of manganese porphyrins bonded to novel modified SBA-15, *New J. Chem.*, 2018, **42**, 6464–6471.
- 47 K. Zhang, O. K. Farha, J. T. Hupp and S. T. Nguyen, Complete double epoxidation of divinylbenzene using Mn (porphyrin)-based porous organic polymers, *ACS Catal.*, 2015, **5**, 4859–4866.
- 48 N. Sharma, S. S. Dhankhar and C. M. Nagaraja, Environment-friendly, co-catalyst and solvent-free fixation of CO₂ using an ionic Zinc(II)-porphyrin complex immobilized in porous metal-organic framework, *Sustainable Energy Fuels*, 2019, **3**, 2977–2982.
- 49 X. Yao, K. Chen, L. Qiu, Z. Yang and L. He, Ferric Porphyrin-Based Porous Organic Polymers for CO₂ Photocatalytic Reduction to Syngas with Selectivity Control, *Chem. Mater.*, 2021, **33**, 8863–8872.
- 50 B. Ugale, S. S. Dhankhar and C. M. Nagaraja, Exceptionally stable and 20-connected lanthanide metal-organic frameworks (MOFs) for selective CO₂ capture and conversion to cyclic carbonates at atmospheric pressure, *Cryst. Growth Des.*, 2018, **18**, 2432–2440.
- 51 D. Chakraborty, S. Nandi, M. A. Sinnwell, J. Liu, R. Kushwaha, P. K. Thallapally and R. Vaidhyanathan, Hyper-Cross-linked Porous Organic Frameworks with Ultramicropores for Selective Xenon Capture, *ACS Appl. Mater. Interfaces*, 2019, **11**, 13279–13284.
- 52 S. Jayakumar, H. Li, J. Chen and Q. Yang, Cationic Zn-Porphyrin Polymer Coated onto CNTs as a Cooperative Catalyst for the Synthesis of Cyclic Carbonates, *ACS Appl. Mater. Interfaces*, 2018, **10**, 2546–2555.
- 53 B.-X. Dong, S.-L. Qian, F.-Y. Bu, Y.-C. Wu, L.-G. Feng, Y.-L. Teng, W.-L. Liu and Z.-W. Li, Electrochemical Reduction of CO₂ to CO by a Heterogeneous Catalyst of Fe-Porphyrin-Based Metal–Organic Framework, *ACS Appl. Energy Mater.*, 2018, **1**, 4662–4669.
- 54 I. Liberman, R. Shimoni, R. Ifraemov, I. Rozenberg, C. Singh and I. Hod, Active-Site Modulation in an Fe-Porphyrin-Based Metal–Organic Framework through Ligand Axial Coordination: Accelerating Electrocatalysis and Charge-Transport Kinetics, *J. Am. Chem. Soc.*, 2020, **142**, 1933–1940.
- 55 R. T. Yang, *Gas Separation by Adsorption Processes*, Butterworth, Boston, 1997.
- 56 H. Pan, J. A. Ritter and P. B. Balbuena, Examination of the Approximations Used in Determining the Isothermic Heat of Adsorption from the Clausius-Clapeyron Equation, *Langmuir*, 1998, **14**, 6323–6327.
- 57 B. Ugale, S. S. Dhankhar and C. M. Nagaraja, Construction of 3-Fold-Interpenetrated Three-Dimensional Metal–

- Organic Frameworks of Nickel(II) for Highly Efficient Capture and Conversion of Carbon Dioxide, *Inorg. Chem.*, 2016, **55**, 9757–9766.
- 58 Y. Gu, B. A. Anjali, S. Yoon, Y. Choe, Y. G. Chung and D.-W. Park, Defect-engineered MOF-801 for cycloaddition of CO₂ with epoxides, *J. Mater. Chem. A*, 2022, **10**, 10051–10061.
- 59 G. Singh and C. M. Nagaraja, Highly efficient metal/solvent-free chemical fixation of CO₂ at atmospheric pressure conditions using functionalized porous covalent organic frameworks, *J. CO₂ Util.*, 2021, **53**, 101716.
- 60 J. F. Kurisingal, Y. Rachuri, A. S. Palakkal, R. S. Pillai, Y. Gu, Y. Choe and D.-W. Park, Water-Tolerant DUT-Series Metal-Organic Frameworks: A Theoretical-Experimental Study for the Chemical Fixation of CO₂ and Catalytic Transfer Hydrogenation of Ethyl Levulinate to γ -Valerolactone, *ACS Appl. Mater. Interfaces*, 2019, **11**, 41458–41471.
- 61 S. S. Dhankhar, R. Das, B. Ugale, R. S. Pillai and C. M. Nagaraja, Chemical Fixation of CO₂ Under Solvent and Co-Catalyst-free Conditions Using a Highly Porous Two-fold Interpenetrated Cu(II)-Metal-Organic Framework, *Cryst. Growth Des.*, 2021, **21**, 1233–1241.
- 62 K. Yu, P. Puthiaraj and W.-S. Ahn, One-pot catalytic transformation of olefins into cyclic carbonates over an imidazolium bromide-functionalized Mn(III)-porphyrin metal-organic framework, *Appl. Catal., B*, 2020, **273**, 119059.
- 63 Q. Han, B. Qi, W. Ren, C. He, J. Niu and C. Duan, Polyoxometalate-based homochiral metal-organic frameworks for tandem asymmetric transformation of cyclic carbonates from olefins, *Nat. Commun.*, 2015, **6**, 10007.
- 64 H. T. D. Nguyen, Y. B. N. Tran, H. N. Nguyen, T. C. Nguyen, F. Gandara and P. T. K. Nguyen, A Series of Metal–Organic Frameworks for Selective CO₂ Capture and Catalytic Oxidative Carboxylation of Olefins, *Inorg. Chem.*, 2018, **57**, 13772–13782.
- 65 L. D. Dias, R. M. B. Carrilho, C. A. Henriques, M. J. F. Calvete, A. M. Masdeu-Bultj, C. Claver, L. M. Rossi and M. M. Pereira, Hybrid Metalloporphyrin Magnetic Nanoparticles as Catalysts for Sequential Transformation of Alkenes and CO₂ into Cyclic Carbonates, *ChemCatChem*, 2018, **10**, 2792–2803.
- 66 N. V. Maksimchuka, I. D. Ivanchikova, A. B. Ayupova and O. A. Kholdeeva, One-step solvent-free synthesis of cyclic carbonates by oxidative carboxylation of styrenes over a recyclable Ti-containing catalyst, *Appl. Catal., B*, 2016, **181**, 363–370.
- 67 N. Sharma, S. S. Dhankhar, S. Kumar, T. J. D. Kumar and C. M. Nagaraja, Rational Design of a 3D Mn^{II}-Metal-Organic Framework Based on a Nonmetallated Porphyrin Linker for Selective Capture of CO₂ and One-Pot Synthesis of Styrene Carbonates, *Chem. – Eur. J.*, 2018, **24**, 16662–16669.
- 68 P. T. K. Nguyen, H. T. D. Nguyen, H. N. Nguyen, C. A. Trickett, Q. T. Ton, E. Gutierrez-Puebla, M. A. Monge, K. E. Cordova and F. Gandara, New Metal-Organic Frameworks for Chemical Fixation of CO₂, *ACS Appl. Mater. Interfaces*, 2018, **10**, 733–744.